Generalized coupling system between a superconducting qubit and two nanomechanical resonators

Feng-Yang Zhang,[1] Wei-Bin Yan,[2,*] and Chui-Ping Yang[3,4,†]
[1]*School of Physics and Materials Engineering, Dalian Nationalities University, Dalian 116600, China*
[2]*College of Physics and Engineering, Qufu Normal University, Qufu 273165, China*
[3]*Quantum Information Research Center, Shangrao Normal University, Shangrao 334001, China*
[4]*Department of Physics, Hangzhou Normal University, Hangzhou 310036, China*

(Received 22 July 2018; published 24 October 2018)

We study a generalized coupling system between a superconducting qubit and two nanomechanical resonators. When the eigenfrequency of the superconducting qubit is twice the frequency of the resonators, we show that one qubit is able to excite simultaneously two resonators. Moreover, tripartite and bipartite macroscopic entangled states are generated, respectively. We give conditions under which general tripartite and bipartite entangled nonorthogonal states become maximally entangled states. Under a large detuning condition, the coupling between two resonators is induced by a superconducting qubit. This coupling strength can be enhanced via a squeezing transformation.

DOI: 10.1103/PhysRevA.98.042331

I. INTRODUCTION

With the rapid development of fabrication techniques, a nanomechanical resonator (NR) is a promising candidate for studying the quantum behavior in mesoscopic mechanical systems, due to frequencies in the gigahertz range [1] and quality factors approaching 10^5 at millidegrees Kelvin temperatures [2,3]. In the past decade, NR has attracted great attention from both theorists and experimentalists. For instance, the superpositions of macroscopically distinct quantum states in a NR have been created and detected [4], the ground-state cooling of a NR has been explored [5–10], a phonon blockade in a NR has been studied [11], quantum entanglement between two NRs has been experimentally demonstrated [12,13], the coupling between NR and several types of matter qubits [superconducting qubits, atoms, or nitrogen-vacancy (NV) centers] has been considered [4,14–20], and quantum information processing with nanomechanical qubits has been proposed [21], and so on.

The flexural modes of thin beams of a NR can be described by the Euler-Bernoulli equations [22]. Its fundamental-mode response can be well described as a damped simple harmonic oscillator with a characteristic resonant frequency ω and effective mass m [23]. After a second quantization, the Hamiltonian can be written as $H_{\mathrm{NR}} = \hbar\omega(a^\dagger a + 1/2)$, where $a^\dagger$ (a) is the phonon creation (annihilation) operator. The fundamental vibrational mode frequencies in the range from 10 MHz to 1 GHz [24,25] and an effective mass $m = 4 \times 10^{-16}$ kg [14] have been fabricated. The quantized nature of the oscillator energy yields an intrinsic fluctuation amplitude, that is, a zero-point uncertainty $\Delta x = \sqrt{\hbar/2m\omega}$. Because of the small mass, a zero-point uncertainty $\Delta x = 2 \times 10^{-14}$ m has been reported [2]. The NR could be a candidate for detecting the transition from classical to quantum noise, because its small mass gives a relatively large zero-point displacement noise [2]. The displacement of the NR results in a linear modulation of the capacitance between the NR and the superconducting qubit [14].

In this paper, we study a hybrid solid quantum model, which consists of a superconducting qubit and two NRs. We find that one qubit is able to excite simultaneously two NRs when the eigenfrequency of the superconducting qubit is twice the frequency of the NRs. When the external magnetic flux is set as $\Phi_e \approx \Phi_0/2$, where Φ_0 is the magnetic-flux quantum, the coupling is longitudinal and the system's parity is conserved. We show that macroscopic tripartite entangled states can be generated by this system. The measurement of the entanglement of nonorthogonal macroscopic tripartite states is demonstrated. Moreover, entangled coherent states of two NRs are obtained by quantum measuring of the superconducting qubit. If the superconducting qubit works near the degenerate point, the system can be described by the Rabi model. When the detuning between the superconducting qubit and the NR is much larger than their coupling strength, the system reduces to the Jaynes-Cummings (JC) model under the rotating-wave approximation. The superconducting qubit can induce the interaction of two NRs.

II. MODEL

We study a hybrid quantum model depicted in Fig. 1, which consists of a superconducting qubit interacting with two NRs via an electrostatic force. Superconducting qubits based on Josephson junctions have recently become the subjects of intense research because they can be designed, fabricated, and controlled for various research purposes [26–29]. Superconducting qubits based on Josephson junctions can basically be divided into four kinds of qubits, called charge, flux, phase, and transmon qubits [28,29]. In this paper, we choose the charge qubit as an example. Also, we can choose the flux,

*yanweibin1983@163.com
†yangcp@hznu.edu.cn

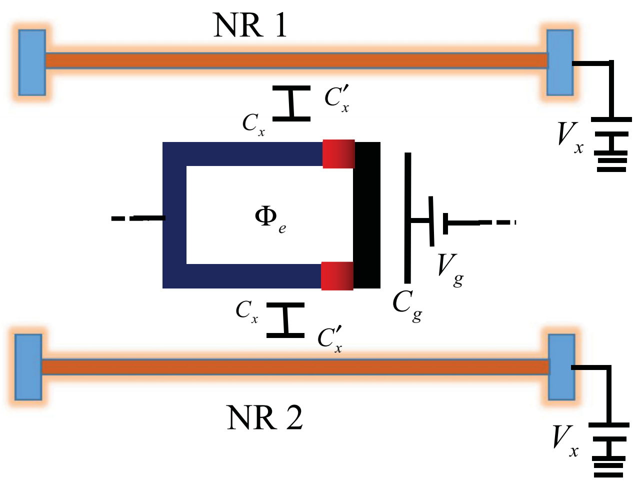

FIG. 1. Schematic diagram of a charge qubit coupled with two nanomechanical resonators (NRs). This superconducting qubit is constructed by two identical Josephson junctions and can be controlled by the gate voltage V_g, gate capacitance C_g, and the external magnetic flux Φ_e. C_x is the coupling capacitance between the charge qubit and the NR. C_x' and V_x are the capacitance and bias voltage of the NR, respectively.

phase, or transmon qubit. The charge qubit is constructed of two identical Josephson junctions with a charging energy E_C, Josephson energy E_J, and Josephson capacitance C_J. It can be controlled by the gate voltage V_g, gate capacitance C_g, and the external magnetic flux Φ_e. The Hamiltonian of a charge qubit is $H_s = -2E_C(1-2n_g)\sigma_z - E_J\cos(\pi\Phi_e/\Phi_0)\sigma_x$ [28], where $n_g = C_gV_g/2e$ is the gate charge, $\sigma_x = |0\rangle\langle 1| + |1\rangle\langle 0|$ and $\sigma_z = |1\rangle\langle 1| - |0\rangle\langle 0|$ are the Pauli matrices, and quantum states $|0\rangle$ and $|1\rangle$ represent zero and one extra Cooper pairs.

The interaction between the charge qubit and the NR is realized via the coupling capacitance C_x. The linear coupling of a NR to a superconducting qubit will produce interesting nonclassical effects [17]. If the distance d between the charge qubit and the NR is much larger than the zero-point uncertainty of the NR Δx, the interaction Hamiltonian is $g(a+a^\dagger)\sigma_z$ [4,14,17], where $g = -2E_CC_xV_x\Delta x/de$ is the capacitive coupling constant with a bias voltage V_x of the NR.

The total Hamiltonian of a charge qubit coupled to two NRs reads ($\hbar = 1$)

$$H = \epsilon\sigma_z - \delta\sigma_x + \sum_{i=1,2}[\omega_i a_i^\dagger a_i + g(a_i^\dagger + a_i)\sigma_z], \tag{1}$$

where the parameters $\epsilon = 2E_C[2(n_g+n_x)-1]$ with a charging energy $E_C = e^2/2(2C_J + C_g + 2C_\Sigma)$, the effective capacitance C_Σ is given by $C_\Sigma = C_xC_x'/(C_x + C_x')$, where C_x' is the capacitance of the NR, $n_x = C_xV_x/2e$, and $\delta = 2E_J\cos(\pi\Phi_e/\Phi_0)$. The first and second terms are free Hamiltonians of the charge qubit. The third term is a free Hamiltonian of two NRs, where ω_i and $a_i^\dagger$ (a_i) are the frequency and phonon creation (annihilation) operators of the ith NR, respectively. The last term represents the interaction Hamiltonian between a charge qubit and two NRs.

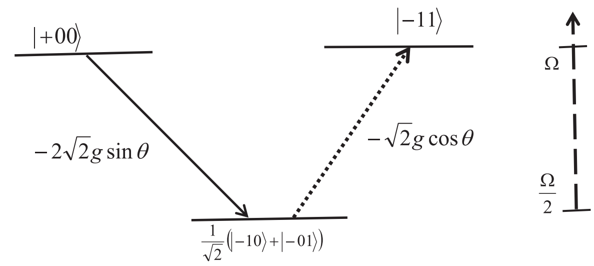

FIG. 2. Transitions between the bare states $|+00\rangle$ and $|-11\rangle$ via an intermediate state $(|-10\rangle + |-01\rangle)/\sqrt{2}$. Here, the excitation-number nonconserving process is represented by the arrowed dashed line.

After transformation to the eigenbasis of the charge qubit, the total Hamiltonian (1) can be written as

$$H = \Omega\tau_z + \sum_{i=1,2}[\omega_i a_i^\dagger a_i + g(a_i^\dagger + a_i)(\cos\theta\tau_z - \sin\theta\tau_x)], \tag{2}$$

where $\Omega = \sqrt{\epsilon^2+\delta^2}$ is the energy-level separation of the charge qubit, and $\tau_x = \tau^+ + \tau^- = |+\rangle\langle -| + |-\rangle\langle +|$ and $\tau_z = |+\rangle\langle +| - |-\rangle\langle -|$ are the Pauli matrices, where the eigenbasis $|+\rangle$ and $|-\rangle$ are defined by $|+\rangle = \cos\theta|0\rangle + \sin\theta|1\rangle$ and $|-\rangle = -\sin\theta|0\rangle + \cos\theta|1\rangle$, respectively. The parameters $\cos\theta = \epsilon/\Omega$ and $\sin\theta = \delta/\Omega$ can be adjusted by the gate voltage V_g, gate capacitance C_g, coupling capacitance C_x, bias voltage V_x, and the external magnetic flux Φ_e. Longitudinal and transverse couplings coexist in this model [30]. Hamiltonian (2) contains counter-rotating terms $a_i^\dagger\tau_z$, $a_i\tau_z$, $a_i^\dagger\tau^+$, and $a_i\tau^-$. The first and second terms create and annihilate one excitation while the last two terms create and annihilate two excitations, respectively. Also, this Hamiltonian describes the system consisting of a two-level atom interacting with double-cavity modes with symmetry-broken potentials.

We investigate the situation where the charge qubit is in the quantum state $|+\rangle$ and the two NRs are initially in the vacuum state $|00\rangle$, corresponding to the initial state $|+00\rangle$ of the system. We find that, if $\Omega \approx 2\omega_i$, a qubit is able to excite simultaneously two NRs, i.e., $|+00\rangle \to |-11\rangle$. The process is shown in Fig. 2, where the initial state $|+00\rangle$ goes to an intermediate state $(|-10\rangle + |-01\rangle)/\sqrt{2}$, and then comes back to the final state $|-11\rangle$. This path includes two transitions involving resonance with the intermediate state. By applying standard perturbation theory, the transition rate can be written as

$$\Gamma_{i\to f} = 2\pi\left|\Xi_{fi}^{\text{eff}}\right|^2\delta(E_f - E_i), \tag{3}$$

where the subscripts i and f represent the initial state $|+00\rangle$ and final state $|-11\rangle$ with corresponding energies E_i and E_f, and Ξ_{fi} is the effective coupling strength between the initial and final states. According to second-order perturbation theory, the effective coupling strength is

$$\Xi_{fi}^{\text{eff}} = \frac{8g^2\sin\theta\cos\theta}{\Omega}, \tag{4}$$

with a perturbation of the form $\Xi = g\sum_{i=1,2}[(a_i^\dagger + a_i)(\cos\theta\tau_z - \sin\theta\tau_x)]$. From Eq. (4), we find that the effective coupling strength Ξ_{fi}^{eff} depends on the mixing angle θ, and it is maximum for $\theta = \pi/4$. We choose the coupling rate $g/\Omega = 0.1$, and an effective Rabi splitting $2\Xi_{fi}^{\text{eff}}/2\pi = 16$ MHz can be obtained for the coupling strength $g/2\pi = 10$ MHz. Reference [31] has discussed that one photon can simultaneously excite two atoms in a quantum system, which constituted two atoms coupled to a single-mode resonator.

III. GENERATION OF MACROSCOPIC ENTANGLED STATES

Under the operating condition of $\Phi_e \approx \Phi_0/2$, the total Hamiltonian (2) becomes

$$H_1 \approx \Omega\tau_z + \sum_{i=1,2}[\omega_i a_i^\dagger a_i + g(a_i^\dagger + a_i)\tau_z]. \tag{5}$$

The system only exists with longitudinal coupling. In the interaction picture, the Hamiltonian of the total system is

$$H_{1,I} = \sum_{i=1,2} g(a_i^\dagger e^{i\omega_i t} + a_i e^{-i\omega_i t})\tau_z. \tag{6}$$

This Hamiltonian describes two NRs that are conditionally displaced by the states of the charge qubit. The unitary evolution operator associated with the Hamiltonian (6) can be expressed as $U(t) = \exp\{i\Lambda(t)\}\exp\{\tau_z\sum_i[\eta_i(t)a_i^\dagger - \eta_i^*(t)a_i]\}$, where $\Lambda(t) = \sum_i (g/\omega_i)^2[\omega_i t - \sin(\omega_i t)]$ is a global phase factor and $\eta_i(t) = (g/\omega_i)(1 - e^{i\omega_i t})$ is the displacement amplitude. Initially, suppose the charge qubit is in a superposition state $(|+\rangle + |-\rangle)/\sqrt{2}$ and the NRs are in the ground state $|0\rangle_1|0\rangle_2$. Hence, the initial state of the system is $|\Psi(0)\rangle = (1/\sqrt{2})(|+\rangle + |-\rangle)|0\rangle_1|0\rangle_2$. By utilizing the unitary evolution operator $U(t)$, the initial state of the total system evolves as

$$|\Psi(t)\rangle = \frac{e^{i\Lambda(t)}}{\sqrt{2}}[|+\rangle|\eta_1(t)\rangle|\eta_2(t)\rangle + |-\rangle|-\eta_1(t)\rangle|-\eta_2(t)\rangle], \tag{7}$$

where $|\eta_i(t)\rangle$ and $|-\eta_i(t)\rangle$ are coherent states of the ith NR $(i = 1, 2)$. Quantum state (7) describes a tripartite entangled state of one charge qubit and two NRs. Thus, this scheme can be applied to generate a tripartite entangled state by a one-step operation. Because the coherent states $|\eta_i(t)\rangle$ and $|-\eta_i(t)\rangle$ are nonorthogonal, quantum state (7) is not a maximal tripartite entangled state. The overlap of two coherent states $|\eta_i(t)\rangle$ and $|-\eta_i(t)\rangle$ is $\exp[-2|\eta_i(t)|^2]$, which decreases exponentially with $|\eta_i(t)|$. For a large enough coherent amplitude $|\eta_i(t)|$, coherent states $|\eta_i(t)\rangle$ and $|-\eta_i(t)\rangle$ are approximately orthogonal. Then, quantum state (7) can be approximated by a tripartite Greenberger-Horne-Zeilinger (GHZ)-like state.

In realistic situations, it is worth investigating the influence of decoherence from the charge qubit and NRs' decay. The dynamics of the system is therefore governed by the following master equation,

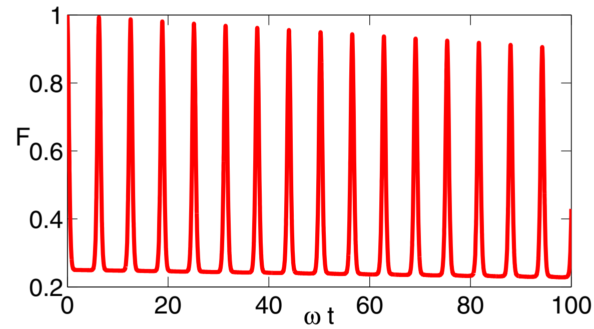

FIG. 3. The fidelity F as function of ωt at $\gamma_1 = \gamma_2 = \kappa_1 = \kappa_2 = 0.001g$. Other parameters are $\omega_1 = \omega_2 = \omega = g$.

$$\dot\rho = i[\rho, H_{1,I}] + \frac{\gamma_1}{2}(\tau_z\rho\tau_z - \rho) + \gamma_2\mathcal{L}[\tau^-]\rho + \sum_{i=1,2}\kappa_i\mathcal{L}[a_i]\rho, \tag{8}$$

where ρ is the density matrix of the system, $\mathcal{L}[o]\rho = o\rho o^\dagger - (o^\dagger o\rho + \rho o^\dagger o)/2$ is the Lindblad superoperator for a given operator o, γ_1 and γ_2 are the pure dephasing and relaxation rates of the charge qubit, respectively, and κ_i is the ith NR decay rate. For an initial state $|\Psi(0)\rangle = (1/\sqrt{2})(|+\rangle + |-\rangle)|0\rangle_1|0\rangle_2$, the master equation (8) can be numerically solved. We can evaluate the generation efficiency of the state (7) by calculating the fidelity $F = \langle\Psi(t)|\rho(t)|\Psi(t)\rangle$. In Fig. 3, we display the time dependence of the fidelity at selected values. The fidelity is a periodic function with ωt. A high-fidelity entangled state can be generated.

Orthogonally tripartite states receive much attention in the study of quantum entanglement [32–34]. A pure three-qubit state entanglement can be measured by three-tangle [32]. However, how can we measure the entanglement of nonorthogonal macroscopic tripartite entangled states? In order to characterize the entanglement of the tripartite quantum state (7), we introduce the even and odd coherent states (the Schrödinger cat states)

$$|\mathbf{1}\rangle_i = M_i^+(|\eta_i(t)\rangle + |-\eta_i(t)\rangle), \tag{9}$$

$$|\mathbf{0}\rangle_i = M_i^-(|\eta_i(t)\rangle - |-\eta_i(t)\rangle), \tag{10}$$

where $M_i^\pm = 1/\sqrt{2(1 \pm e^{-2|\eta_i(t)|^2})}$ are normalization coefficients. One can also use Schrödinger cat states to encode a qubit and they are exactly orthogonal. Under the Schrödinger cat state representation, quantum state (7) can be rewritten as

$$|\Psi(t)\rangle = \frac{e^{i\Lambda(t)}}{4}\bigg(\frac{1}{M_1^+M_2^+}|1\rangle|\mathbf{1}\rangle_1|\mathbf{1}\rangle_2 + \frac{1}{M_1^+M_2^-}|0\rangle|\mathbf{1}\rangle_1|\mathbf{0}\rangle_2 + \frac{1}{M_1^-M_2^+}|0\rangle|\mathbf{0}\rangle_1|\mathbf{1}\rangle_2 + \frac{1}{M_1^-M_2^-}|1\rangle|\mathbf{0}\rangle_1|\mathbf{0}\rangle_2\bigg). \tag{11}$$

Equation (11) is an exactly orthogonal tripartite entangled state. Then, the entanglement can be measured by three-tangle. For a tripartite pure state of qubits, $|\psi\rangle =$

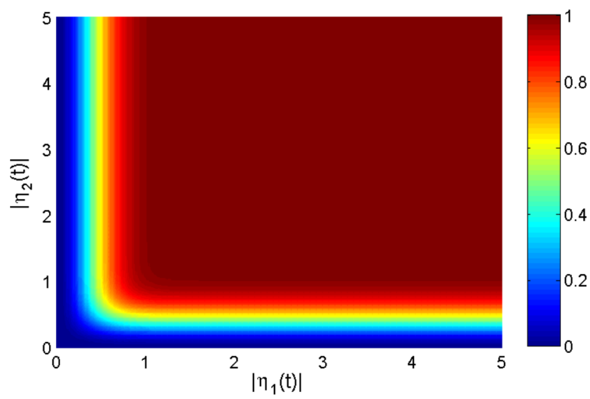

FIG. 4. Three-tangle $T(t)$ with the coherent amplitudes $|\eta_1(t)|$ and $|\eta_2(t)|$.

$\sum_{i,j,k=0}^{1} a_{ijk}|ijk\rangle$, the three-tangle can be given by [32]

$$T = 4|d_1 - 2d_2 + 4d_3|, \tag{12}$$

with

$$\begin{aligned} d_1 &= a_{000}^2 a_{111}^2 + a_{001}^2 a_{110}^2 + a_{010}^2 a_{101}^2 + a_{100}^2 a_{011}^2, \\ d_2 &= a_{000}a_{111}a_{011}a_{100} + a_{000}a_{111}a_{101}a_{010} \\ &\quad + a_{000}a_{111}a_{110}a_{001} + a_{011}a_{100}a_{101}a_{010} \\ &\quad + a_{011}a_{100}a_{110}a_{001} + a_{101}a_{010}a_{110}a_{001}, \\ d_3 &= a_{000}a_{110}a_{101}a_{011} + a_{111}a_{001}a_{010}a_{100}. \end{aligned} \tag{13}$$

Therefore, the three-tangle of the quantum state (11) is

$$T(t) = \left(1 - e^{-4|\eta_1(t)|^2}\right)\left(1 - e^{-4|\eta_2(t)|^2}\right). \tag{14}$$

In Fig. 4, we plot the three-tangle $T(t)$ with the coherent amplitudes $|\eta_1(t)|$ and $|\eta_2(t)|$. We can see that the entanglement can be enhanced with increasing both $|\eta_1(t)|$ and $|\eta_2(t)|$. According to the expression of coherent amplitude $|\eta_i(t)| = (2g/\omega_i)\sin(\omega_i t/2)$, we can see that the three-tangle can be changed by the g/ω_i and $\omega_i t$. In Fig. 5(a), we plot the three-tangle $T(t)$ with the $\omega_1 t$ and $\omega_2 t$ for the coupling rate $g/\omega_i = 1$. Figure 5(b) shows the three-tangle $T(t)$ with the $\omega_1 t$ and $\omega_2 t$ for the coupling rate $g/\omega_i = 0.5$. We can see that the entanglement is a periodic function of $\omega_i t$. When the evolution time takes $t = 2n\pi/\omega_i$ for a natural number n, the coherent amplitude is zero, i.e., $|\eta_i(t)| = 0$. At this moment, the charge qubit and the NRs are decoupling and the entanglement disappears. Also, comparing with Figs. 5(a) and 5(b), the three-tangle depends on the coupling rate g/ω_i, due to the fact that the coherent amplitude $|\eta_i(t)|$ is in direct proportion to the coupling rate g/ω_i. For a large enough coupling rate g/ω_i, the coherent states $|\eta_i(t)\rangle$ and $|-\eta_i(t)\rangle$ are approximatively orthogonal.

We change the basis states of the charge qubit to optional basis states $|\mu\rangle = \sin\vartheta|+\rangle + \cos\vartheta|-\rangle$ and $|\nu\rangle = \cos\vartheta|+\rangle - \sin\vartheta|-\rangle$ with parameter ϑ, and quantum state (7) is written as

$$|\Psi(t)\rangle = e^{i\Lambda(t)}[|\alpha_-(t)\rangle|\nu\rangle + |\alpha_+(t)\rangle|\mu\rangle], \tag{15}$$

where $|\alpha_-(t)\rangle = (\cos\vartheta|\eta_1(t)\rangle|\eta_2(t)\rangle - \sin\vartheta|-\eta_1(t)\rangle|-\eta_2(t)\rangle)/\sqrt{2}$ and $|\alpha_+(t)\rangle = (\sin\vartheta|\eta_1(t)\rangle|\eta_2(t)\rangle + \cos\vartheta|-\eta_1(t)\rangle|-\eta_2(t)\rangle)/\sqrt{2}$ are entangled coherent states. If we measure the charge qubit in the basis $\{|\mu\rangle, |\nu\rangle\}$, the quantum state of two NRs collapses into $|\alpha_-(t)\rangle$ or $|\alpha_+(t)\rangle$. That is to say, macroscopic entangled states of two NRs can be generated by this scheme.

Quantum states $|\alpha_-(t)\rangle$ and $|\alpha_+(t)\rangle$ are bipartite entangled nonorthogonal states. The concurrence for bipartite entangled nonorthogonal states has been studied [35,36]. Therefore, the concurrence for $|\alpha_\pm(t)\rangle$ is given by

$$C_\pm(t) = \frac{|\sin(2\vartheta)|\sqrt{(1-e^{-4|\eta_1(t)|^2})(1-e^{-4|\eta_2(t)|^2})}}{1 \pm e^{-2(|\eta_1(t)|^2+|\eta_2(t)|^2)}|\sin(2\vartheta)|}. \tag{16}$$

We plot the concurrence $C_+(t)$ of the even entangled coherent state with $\omega_1 t$ and $\omega_2 t$ in Fig. 6(a), and the concurrence $C_-(t)$ of the odd entangled coherent state with $\omega_1 t$ and $\omega_2 t$ is shown in Fig. 6(b). We can see that the entanglement is a periodic function of $\omega_i t$, but the entanglement of two kinds of entangled coherent states presents different behaviors for a different $\omega_i t$.

IV. ENHANCED COUPLING OF TWO NRs

If the charge qubit works near the degenerate point, the total Hamiltonian becomes

$$H_2 \approx \Omega\tau_z + \sum_{i=1,2}[\omega_i a_i^\dagger a_i + g(a_i^\dagger + a_i)\tau_x]. \tag{17}$$

The system only exists with transverse coupling. In the interaction picture, under the rotating-wave approximation the

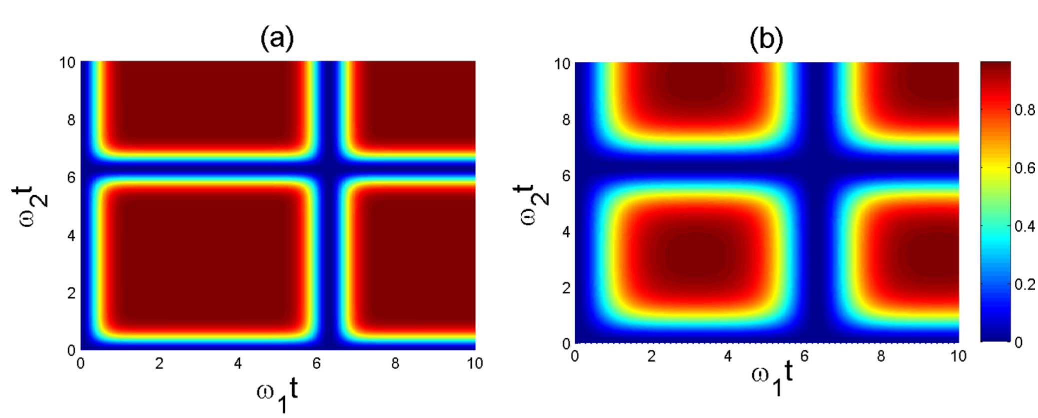

FIG. 5. Three-tangle $T(t)$ with $\omega_1 t$ and $\omega_2 t$ for different cases: (a) $g/\omega_i = 1$, (b)$g/\omega_i = 0.5$.

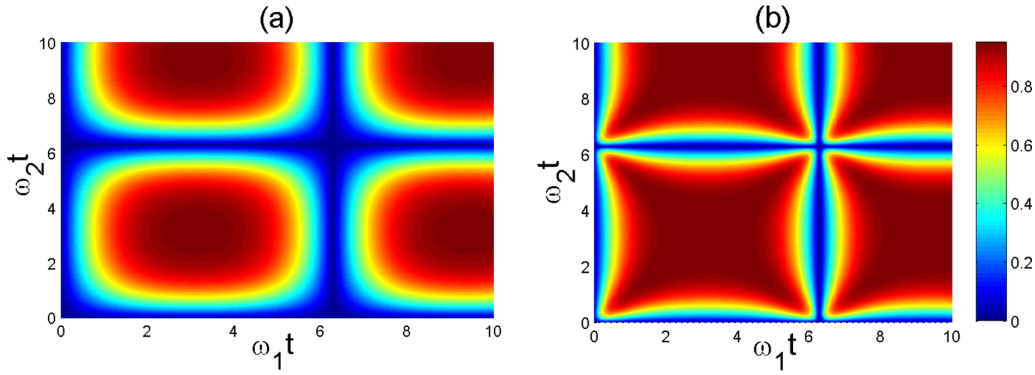

FIG. 6. Concurrence of the entangled coherent states $|\alpha_{\pm}(t)\rangle$ with $\omega_1 t$ and $\omega_2 t$, where we set $\sin(2\vartheta) = 0.95$ and $g/\omega_i = 1$. (a) is for an even entangled coherent state and (b) is for an odd entangled coherent state.

Hamiltonian (16) can be written as

$$H_{2,I} = \sum_{i=1,2} g(e^{i\Delta_i t} a_i \tau^+ + \text{H.c.}), \tag{18}$$

where $\Delta_i = \Omega - \omega_i$ is the detuning between the charge qubit and the ith NR. Under the large-detuning condition $|\Delta_i| \gg g$ and when the superconducting qubit is prepared in the quantum state $|-\rangle$, the Hamiltonian of Eq. (18) can be expressed as the following effective Hamiltonian [37],

$$H_{2,e} = \frac{g^2}{\Delta_1} a_1^\dagger a_1 + \frac{g^2}{\Delta_2} a_2^\dagger a_2 + \lambda\big(a_2^\dagger a_1 e^{i(\Delta_1 - \Delta_2)t} + \text{H.c.}\big), \tag{19}$$

where the first two terms describe the phonon-number-dependent Stark shifts, and the third term represents the interaction of two NRs with the coupling strength $\lambda = \frac{g^2}{2}(\frac{1}{\Delta_1} + \frac{1}{\Delta_2})$. So, the coupling strength of two NRs can be adjusted by changing the parameters g_1, g_2, Δ_1, or Δ_2. For a simple case, we choose $\Delta_1 = \Delta_2 = \Delta$, and we choose $g = 0.1\Delta$ to satisfy the large detuning condition. We consider a NR with frequency $\omega/2\pi = 1 \times 10^2$ MHz [3,6,38]. For the charge qubit, a Josephson energy of $E_J/2\pi = 2 \times 10^4$ MHz and charging energy $E_C/2\pi = 6.4 \times 10^4$ MHz were considered in Refs. [6,38]. If the distance between the charge qubit and the NR is $d = 100$ nm, the coupling strength is evaluated as $g/2\pi = 10$ MHz [6,38]. Therefore, the effective coupling strength of two NRs can be estimated as $\lambda/2\pi = 1$ MHz. Apparently, this coupling coefficient is much larger than the decay rate $\kappa/2\pi = 0.5 \times 10^{-3}$ MHz of the NR [6]. This implies that two NRs can be strongly coupled together via a charge qubit.

We introduce the squeezing transformation $a_i = d_i \cosh(r) - d_i^\dagger \sinh(r)$ with the squeeze parameter $r = g/\Delta$ [39]. Then, we choose $\Delta_1 = \Delta_2 = \Delta$, and the Hamiltonian (19) is written as

$$\widetilde{H}'_{2,e} = \sum_{i=1,2} \big[\chi_1 d_i^\dagger d_i - \chi_2\big(d_i^{\dagger 2} + d_i^2\big)\big] + \lambda_c(d_2^\dagger d_1 + d_1^\dagger d_2) - \lambda_s(d_1^\dagger d_2^\dagger + d_1 d_2), \tag{20}$$

where the first term describes the free Hamiltonian of two NRs with an effective frequency $\chi_1 = (g^2/\Delta)\cosh(2r)$, the second term is two-phonon parametric driving with a drive amplitude $\chi_2 = (g^2/2\Delta)\sinh(2r)$, the third term is a single-phonon exchange process of two NRs with a transformed coupling strength $\lambda_c = \lambda\cosh(2r)$, and the last term is the two-phonon process with a coupling strength $\lambda_s = \lambda\sinh(2r)$. Figure 7 shows that the relative coupling strength λ_c/λ can be enhanced by increasing the squeeze parameter $r = g/\Delta$. Because of the parametric-driving-induced squeezing to NRs, the single-phonon state corresponds to an increased number of phonons compared to the original mode.

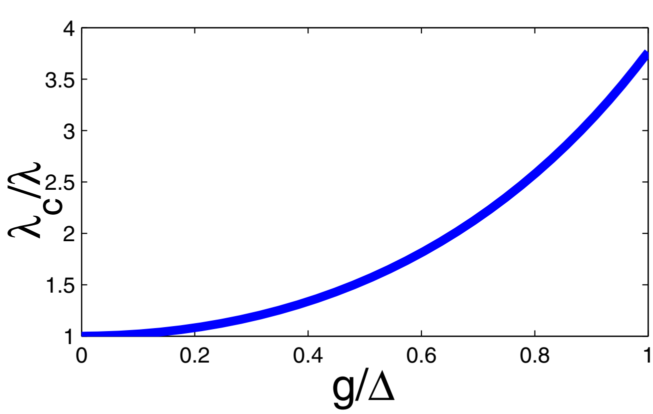

FIG. 7. The relative coupling strength λ_c/λ with squeeze parameter $r = g/\Delta$.

V. DISCUSSIONS AND CONCLUSIONS

It is very interesting to discuss whether our proposal can be realized in current experimental setups. The coupling between a charge qubit and a NR has been reported [4,6,14,15,38]. The NR is formed from low-stress silicon nitride with a thin coating of aluminum, and the superconducting qubit is formed from aluminum during the same deposition steps as the nanoresonator [14]. In order to generate stabled macroscopic entangled states, we require a large enough coupling rate g/ω_i. On the other hand, when the superconducting qubit can induce the coupling between two NRs, the large detuning condition $|\Delta_i| \gg g$ should be satisfied, so that the coupling rate $g/\omega_i < 1$. A recent experiment has reported that a coupling rate g/ω_i of the superconducting qubit and the resonator, ranging from 0.72 to 1.34, has been realized [40].

We note that this proposal could be used to achieve quantum information transfer and quantum logic gates between the two NRs. In general, qubits are encoded in two-level systems, such as atoms, photons, and solid systems. Here, a qubit is encoded in the high-dimensional space of a NR, rather than in a two-level system. The main advantage of this encoding is robust to the single-particle loss. A recent experiment has implemented a controlled-NOT (CNOT) gate between multiphoton encoding qubits in two cavities [41].

In conclusion, we have studied a solid quantum device composed of a superconducting qubit and two NRs. We found that one qubit is able to excite simultaneously two resonators. When the system only exists with longitudinal coupling, the generation and measurement of tripartite and bipartite macroscopic entangled states have been discussed. When the system only exists with transverse coupling, the interaction of two NRs can be induced by a superconducting qubit, and this coupling strength of two NRs can be enhanced via parametric-induced squeezing. Moreover, we have justified the experimental feasibility and challenges using currently available technology.

ACKNOWLEDGMENTS

F.-Y.Z. thanks Professor Jia-Sen Jin for discussions. F.-Y.Z. was supported by the National Science Foundation of China under Grants No. 11505024 and No. 11447135, the Natural Science Foundation of Liaoning Province under Grant No. 20180550944, and the Fundamental Research Funds for the Central Universities Grant No. wd01151. W.-B.Y. was supported by the National Science Foundation of China under Grants No. 11505023 and No. 11447134. C.-P.Y. was supported in part by the NKRDP of China under Grant No. 2016YFA0301802, and the National Natural Science Foundation of China under Grants No. 11074062, No. 11374083, and No. 11774076.

[1] X. M. H. Huang, C. A. Zorman, M. Mehregany, and M. L. Roukes, Nature (London) **421**, 496 (2003).
[2] R. G. Knobel and A. N. Cleland, Nature (London) **424**, 291 (2003).
[3] M. D. LaHaye, O. Buu, B. Camarota, and K. C. Schwab, Science **304**, 74 (2004).
[4] A. D. Armour, M. P. Blencowe, and K. C. Schwab, Phys. Rev. Lett. **88**, 148301 (2002).
[5] I. Martin, A. Shnirman, L. Tian, and P. Zoller, Phys. Rev. B **69**, 125339 (2004).
[6] P. Zhang, Y. D. Wang, and C. P. Sun, Phys. Rev. Lett. **95**, 097204 (2005).
[7] Y. D. Wang, Y. Li, F. Xue, C. Bruder, and K. Semba, Phys. Rev. B **80**, 144508 (2009).
[8] J. P. Zhu and G. X. Li, Phys. Rev. A **86**, 053828 (2012).
[9] P. Stadler, W. Belzig, and G. Rastelli, Phys. Rev. Lett. **117**, 197202 (2016).
[10] I. Wilson-Rae, P. Zoller, and A. Imamoğlu, Phys. Rev. Lett. **92**, 075507 (2004).
[11] Y. X. Liu, A. Miranowicz, Y. B. Gao, J. Bajer, C. P. Sun, and F. Nori, Phys. Rev. A **82**, 032101 (2010).
[12] C. F. Ockeloen-Korppi, E. Damskägg, J.-M. Pirkkalainen, M. Asjad, A. A. Clerk, F. Massel, M. J. Woolley, and M. A. Sillanpää, Nature (London) **556**, 478 (2018).
[13] R. Riedinger, A. Wallucks, I. Marinković, C. Löschnauer, M. Aspelmeyer, S. Hong, and S. Gröblacher, Nature (London) **556**, 473 (2018).
[14] M. D. LaHaye, J. Suh, P. M. Echternach, K. C. Schwab, and M. L. Roukes, Nature (London) **459**, 960 (2009).
[15] G. Chen, Z. Chen, L. Yu, and J. Liang, Phys. Rev. A **76**, 024301 (2007).
[16] X. Zhou and A. Mizel, Phys. Rev. Lett. **97**, 267201 (2006).
[17] E. K. Irish and K. Schwab, Phys. Rev. B **68**, 155311 (2003).
[18] P. Treutlein, D. Hunger, S. Camerer, T. W. Hänsch, and J. Reichel, Phys. Rev. Lett. **99**, 140403 (2007).
[19] P. Rabl, P. Cappellaro, M. V. G. Dutt, L. Jiang, J. R. Maze, and M. D. Lukin, Phys. Rev. B **79**, 041302(R) (2009).
[20] P. B. Li, Z. L. Xiang, P. Rabl, and F. Nori, Phys. Rev. Lett. **117**, 015502 (2016).
[21] S. Rips and M. J. Hartmann, Phys. Rev. Lett. **110**, 120503 (2013).
[22] A. N. Cleland, *Foundations of Nanomechanics* (Springer, Berlin, 2002).
[23] A. D. Armour and M. P. Blencowe, Phys. Rev. B **64**, 035311 (2001).
[24] A. N. Cleland and M. L. Roukes, Appl. Phys. Lett. **69**, 2653 (1996).
[25] D. W. Carr, S. Evoy, L. Sekaric, H. G. Craighead, and J. M. Parpia, Appl. Phys. Lett. **75**, 920 (1999).
[26] Y. Makhlin, G. Schön, and A. Shnirman, Rev. Mod. Phys. **73**, 357 (2001).
[27] J. Clarke and F. K. Wilhelm, Nature (London) **453**, 1031 (2008).
[28] J. Q. You and F. Nori, Phys. Today **58** (11), 42 (2005); Nature (London) **474**, 589 (2011).
[29] X. Gu, A. F. Kockum, A. Miranowicz, Y. X. Liu, and F. Nori, Phys. Rep. **718-719**, 1 (2017).
[30] R. Stassi and F. Nori, Phys. Rev. A **97**, 033823 (2018).
[31] L. Garziano, V. Macrì, R. Stassi, O. DiStefano, F. Nori, and S. Savasta, Phys. Rev. Lett. **117**, 043601 (2016).
[32] V. Coffman, J. Kundu, and W. K. Wootters, Phys. Rev. A **61**, 052306 (2000).
[33] X. J. Ren, Z. Wang, X. Zhou, Z. W. Zhou, and L. He, Phys. Rev. A **81**, 042306 (2010).
[34] C. S. Yu and H. S. Song, Phys. Rev. A **76**, 022324 (2007).
[35] X. G. Wang, J. Phys. A **35**, 165 (2002); F. Y. Zhang, C. P. Yang, X. L. He, and H. S. Song, Phys. Lett. A **378**, 1536 (2014).
[36] M. Y. Chen, M. W. Y. Tu, and W. M. Zhang, Phys. Rev. B **80**, 214538 (2009).
[37] D. F. James and J. Jerke, Can. J. Phys. **85**, 625 (2007).
[38] G. Chen, Z. Chen, J. Li, and J. Liang, Phys. Rev. B **75**, 212508 (2007).
[39] D. F. Walls and G. J. Milburn, *Quantum Optics* (Springer, Berlin, 1994).
[40] F. Yoshihara, T. Fuse, S. Ashhab, K. Kakuyanagi, S. Saito, and K. Semba, Nat. Phys. **13**, 44 (2017).
[41] S. Rosenblum, Y. Y. Gao, P. Reinhold, C. Wang, C. J. Axline, L. Frunzio, S. M. Girvin, L. Jiang, M. Mirrahimi, M. H. Devoret, and R. J. Schoelkopf, Nat. Commun. **9**, 652 (2018).